Saturation of optical absorption by a nonequilibrium electron-hole plasma in InSb crystals

P. Lavallard, R. Bichard, and C. Benoît à la Guillaume
Groupe de Physique des Solides de l'ENS, Tour 23, Université Paris VII, 2 Place Jussieu, 75005 Paris, France*
(Received 26 July 1976)

A high degree of saturation of optical absorption in InSb is observed at 2°K by using several lines (between 5.5 and 5 μm) of a cw CO laser. Luminescence is studied in the same conditions. A model of dynamic Burstein shift is presented which allows us to fit both theoretical transmission and luminescence with the data by taking into account band-gap renormalization and carrier heating. We emphasize that the principal experimental uncertainties arise from inhomogeneous pumping and interference effects in the sample. We show that a weak transverse magnetic field reduces the transmission of circularly polarized light.

I. INTRODUCTION

In semiconductors, one may obtain saturation of optical absorption at least by three mechanisms: (i) self-induced transparency, where a powerful light pulse, of duration shorter than the relaxation times, can propagate as a result of induced reradiation of the medium[1,2]; (ii) saturation of the absorption between two electronic bands in a two-level model, where a monochromatic light beam generates enough carriers to fill band states related by the optical transition; in this case, the carrier distribution cannot be described by an effective temperature (hole-burning model)[3]; and (iii) dynamic Burstein shift, which occurs when enough carriers are generated by light to fill band states up to and including those of the optical transition.[4]

Saturation of the band-to-band transition has been obtained in several semiconductors: GaAs,[5] $InAs_xP_{1-x}$,[6] $Ga_{1-x}In_xAs$,[6] InSb,[7] $Hg_xCd_{1-x}Te$,[8] and Ge,[9] with pulsed lasers of high power. In these experimental conditions, it is not always obvious that the invoked mechanism, i.e., dynamic Burstein shift or hole burning is the cause of saturation.

We present here results of optical-absorption saturation in InSb obtained with a cw CO laser at low intensity (~100 W/cm^2).[10] Transmission of the laser beam and luminescence of the sample are studied at pumped-helium temperature. We show that the dynamic-Burstein-shift model explains satisfactorily the experimental results. The principal uncertainties arise from inhomogeneity of the laser-beam intensity and interferences between the two faces of the sample. Values of electronic temperature, photoexcited carriers lifetime, and band-gap renormalization energy are discussed. We show that a weak transverse magnetic field reduces the transmission of circularly polarized light and discuss the effect of band filling on the creation of electronic polarization by optical pumping.

II. EXPERIMENTS

A. Results

The experiments are performed on several InSb samples ($n = 2 \times 10^{14}$ cm^{-3} and $p = 2.6 \times 10^{15}$ cm^{-3} at 77°K) immersed in pumped helium. Their surfaces is large enough to obtain a good thermal contact with helium bath and avoid formation of helium gas bubbles by laser heating. In order to avoid self-mode locking and erratic pulses, the cavity of the CO laser is apertured; its length is adjusted by a piezoelectric crystal monitored by an electronic loop so that the laser works on a single mode. The laser beam is focused by a CaF_2 lens (focal length: 10 cm) into a 0.2-mm-diam spot on the sample. The power of the laser is monitored by changing the discharge current. We use several spectral lines of the CO laser with photon energy ranging from the InSb band-gap energy ($E_G^0 = 235$ meV) to 241 meV. The transmitted light passes through a monochromator and is focused on a liquid-nitrogen-cooled PbSe cell. A small amount of the laser power split off by partial reflexion on a CaF_2 plate and focused on a InSb diode, gives a relative measurement of the incident power. The linearity of the detection system is tested without a sample. For absolute measurements, we use a Moll thermopile calibrated with a power meter. The luminescence is collected from the front face of the sample and focused on the monochromator entrance slit by an elliptical mirror.

Figure 1 shows the transmitted power versus the incident power for several lines of the CO laser. The thickness d of the sample is 60 μm. For sufficiently high incident power, the transmitted power varies linearly with the incident power. The interception of the straight line with the incident power axis determines the threshold power necessary to achieve almost totally the saturation of optical absorption. The threshold increases with the laser photon energy, as can be seen in

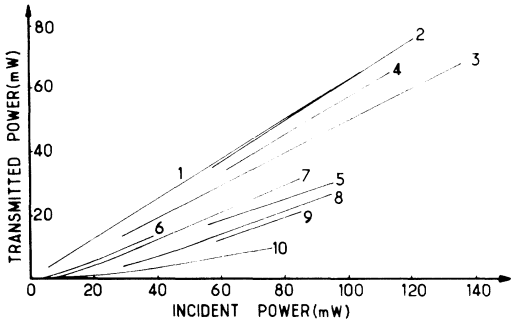

FIG. 1. Transmitted power vs the incident power for several lines of the CO laser: 230.3 meV (1), 232.3 meV (2), 235 meV (3), 235.5 meV (4), 236 meV (5), 236.5 meV (6), 237.2 meV (7), 238.2 meV (8), 238.6 meV (9) 239.1 meV (10). Sample is 60 μm thick. Incident power is varied by changing discharge current. Constructive interferences are carried out to obtain reproducible measurements (see the text). Maximum transmitted and incident power are measured in absolute value with a thermopile. No correction for Dewar-window transmission is done.

Fig. 2. For the highest incident powers used here (~0.1 W) we measure a rate of transmission which is 0.3 to 0.9 times the rate of transmission observed at a photon energy lower than the band-gap energy.

Furthermore, by superimposing to the CO laser beam a YAlG laser beam ($\lambda = 1.06$ μm), we observe an enhancement of the CO line transmission. Since the photon energies of the two beams are different, self-induced transparency or hole-burning mechanisms cannot explain our result. We conclude that the CO line transmission is enhanced by the filling of states near the surface where the YAlG photons are absorbed.

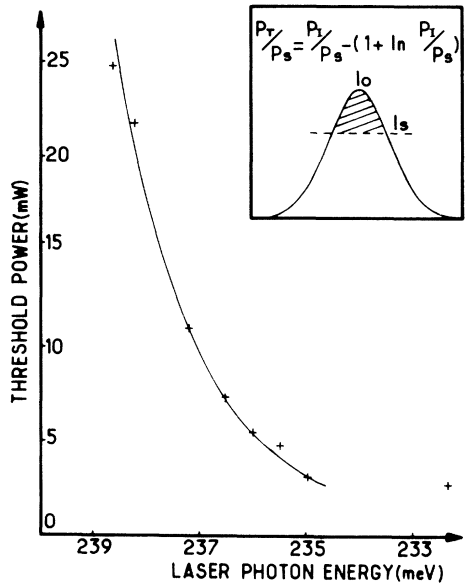

FIG. 2. Threshold power dependence on laser photon energy. The shaded area in the inset is the transmitted power for a Gaussian distribution in intensity in the laser spot. I_s is the threshold intensity; the corresponding threshold power P_s is multiplied by $(1+\ln P_I/P_s)$ when the intensity distribution is taken into account.

Fluorescence is studied in the same conditions of optical absorption saturation. Figure 3 shows a typical band-to-band recombination line, obtained with the $h\nu = 238.6$-meV CO line. The spectrum indicates that the energy gap has a value close to $E_G = 232.5$ meV as compared to the value 234 meV deduced from recombination radiation spectrum obtained with excitation by high-pressure mercury lamp.[11] This band-gap shift is attributed (as discussed below) to exchange and correlation energies between carriers. Furthermore, we observe a low-energy tail (not shown in Fig. 3), which can be described as a plasmon sideband.[12] The spectrum does not extend up to the laser line energy. This is well explained by taking into account gain at low-photon energy and reabsorption at high-photon energy, as shown in theoretical part.

B. Discussion

As clearly seen in Fig. 4, the transmission rate is strongly dependent on the laser spot position on the sample. By translating the sample continuously, we obtain successively maxima and minima of transmission. Besides we observe on the band-to-band recombination line a structure which depends correlatively on the laser-spot position. For example, in Fig. 3, one can see two maxima

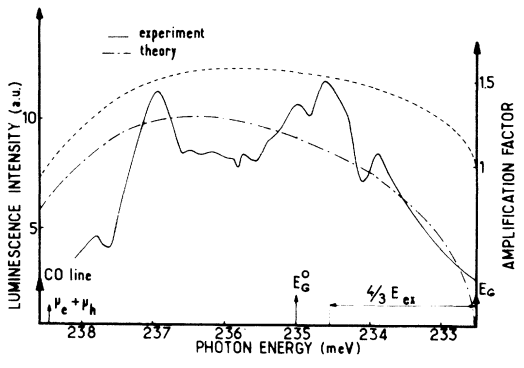

FIG. 3. Band-to-band recombination spectrum of p-type InSb ($p \sim 2.6\times10^{15}$ cm^{-3}) at pumped helium temperature. The sample thickness is 60 μm; the source is a cw CO laser ($h\nu = 238.6$ meV, $P_I = 80$ mW). Arrows indicate the optical band-gap energy E_G and the sum of electron and hole quasi-Fermi energies, $\mu_e + \mu_h$. The effective carrier temperature is 10 °K.

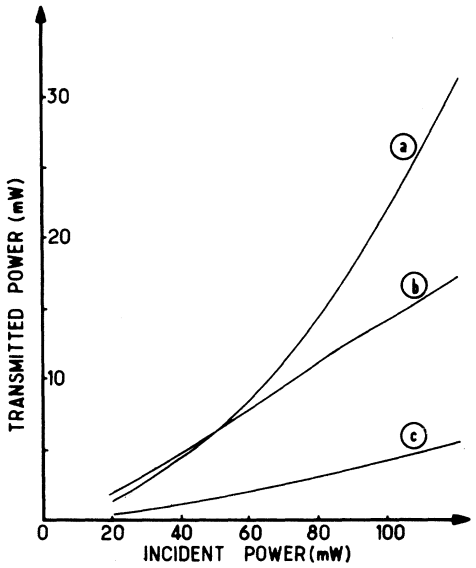

FIG. 4. Transmitted power vs incident power for the CO line, $h\nu = 238.2$ meV. The a, b, c curves are obtained for different positions of the laser spot on the sample.

at $h\nu = 236.9$ meV and $h\nu = 234.6$ meV. (Dips are due to the atmospheric water vapor absorption.) We interpret these facts as a Fabry-Perot interference between not strictly parallel faces of the sample.[13] In order to take all of the transmission measurements (Fig. 1) under the same conditions, constructive interferences are achieved as best as possible by slightly moving the sample with respect to the laser spot.

Furthermore, we must take into account the spatial distribution of the intensity in the laser spot. The divergence of the laser beam is evaluated to be 2 mrad. The corresponding focused spot diameter (0.2 mm) is of the same order of magnitude as the diffraction spot diameter. Even at high power, saturation of absorption is not achieved in the tail of the distribution. The effect of the laser-spot inhomogeneity is particularly clear on the conduction-band–to–acceptor line. Since the number of neutral acceptors is roughly independent of the intensity of the excitation,[14] the integrated intensity of the line is proportional to the stationary number of photoexcited electrons. Even for the highest powers of laser lines, the band-acceptor line intensity does not saturate but shows a nearly logarithmic dependence on the CO line intensity (Fig. 5).

The effect of the laser-spot inhomogeneity modifies the value of the observed threshold power. For high-incident intensity I_I, the transmitted intensity I_T is

$$I_T = I_I - I_S \ , \tag{1}$$

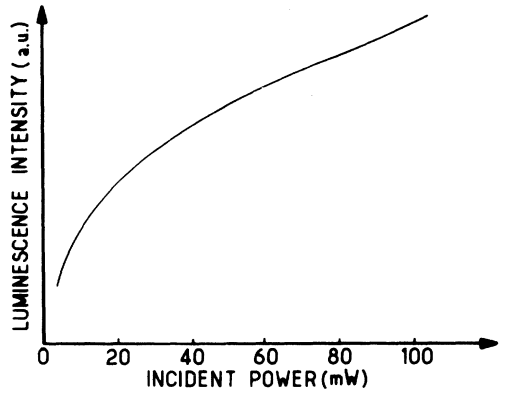

FIG. 5. Luminescence intensity of the acceptor line vs the incident power for the CO line, $h\nu = 238.2$ meV.

where I_S is the threshold intensity. Assuming a Gaussian distribution of intensity in the laser spot, one sees that the transmitted power P_T (shaded area of the insert of Fig. 2) is given by

$$P_T/P_S = P_I/P_S - \left[1 + \ln\left(\frac{P_I}{P_S}\right)\right] , \tag{2}$$

where P_I is the incident power and $P_I/P_S = I_I/I_S$.

The interception of the straight line for values of I_I/I_S up to 8–9 gives an apparent threshold value two times greater than P_S. As can be seen from Eq. (2), the slope of the transmission curves is always less than one. The slope value is smaller when extrapolation is done closer to the threshold.

III. THEORY

We assume that the exciting laser beam is homogeneous and neglect the Fabry-Perot interferences. We take a mean band gap independent of carrier concentration. This last assumption is not important for thin samples in which carrier concentration is almost homogeneous.

The main mechanism of carrier recombination at low temperature for densities of interest here ($n \sim 10^{15}$ cm^{-3}) is the radiative recombination.[15]

For a steady light beam corresponding to a photon flux density J travelling in the x direction, we can write

$$-\frac{dJ}{dx} = \alpha(x)J(x) = r[n(x)]^2 \ , \tag{3}$$

where r is the bimolecular constant of radiative recombination[16] and α the absorption coefficient. The hole density is taken equal to the electron density. We assume that the hole temperature is equal to the electron temperature (T). This is justified since in our experimental conditions the rate of electronic energy loss by electron-hole scattering $1/\tau_\epsilon$ (Ref. 17) is much larger than the

rate of radiative recombination of photoexcited carriers.

The optical absorption coefficient α for direct transitions between the conduction band and the two upper valence bands can be written

$$\alpha(h\nu)=\frac{\alpha_0(h\nu)}{1+(\mu_{1h}/\mu_{hh})^{3/2}}\left\{\left[1-f_e\left(\eta\,\frac{\mu_{hh}}{m_e}\right)-f_h\left(\eta\,\frac{\mu_{hh}}{m_h}\right)\right]+\left(\frac{\mu_{1h}}{\mu_{hh}}\right)^{3/2}\left[1-f_e\left(\eta\,\frac{\mu_{1h}}{m_e}\right)-f_h\left(\eta\,\frac{\mu_{1h}}{m_h}\right)\right]\right\}, \quad (4)$$

where $\eta=(h\nu-E_G)/kT$, $\mu_{hh}=m_e m_{hh}/(m_e+m_{hh})$, $\mu_{1h}=m_e m_{1h}/(m_e+m_{1h})m_e$, m_{1h}, m_{hh} are effective masses for electrons, light holes, and heavy holes, respectively. k is the Boltzmann constant. f_e and f_h are the Fermi distributions of electrons in the conduction band and holes in the valence bands. α_0 is the absorption coefficient at low intensity. The electronic density is

$$n(x)=4\pi(2m_e kT/h^2)^{3/2}F_{1/2}(\xi_e(x)) . \quad (5)$$

$\xi_e(x)$ is the quasi-Fermi energy of electrons in units of kT at a depth x. $F_{1/2}(\xi)$ is the well-known Fermi integral $\int_0^\infty \eta^{1/2} f(\eta,\xi)\,d\eta$. The hole quasi-Fermi energy $\xi_h(x)$ is related to $\xi_e(x)$ by writing the equality of electron and hole densities.

Combining these equations, we obtain

$$\alpha_0 x=\int_{\xi_e(x)}^{\xi_e(0)}\frac{1}{[F_{1/2}(\xi_e)]^2}\,d\left(\frac{[F_{1/2}(\xi_e)]^2}{\alpha_0/\alpha_0}\right), \quad (6)$$

$$J(x)=16\pi^2\left(\frac{2m_e kT}{h^2}\right)^3\frac{r}{\alpha_0}\left(\frac{[F_{1/2}(\xi_e)]^2}{\alpha/\alpha_0}\right)_x . \quad (7)$$

The electronic temperature is determined by the equilibrium between powers received and lost by the electron-hole plasma

$$\frac{h\nu-E_G}{\tau_{rad}}=\frac{kT}{T_{rad}}\left(\frac{F_{3/2}(\xi_e)}{F_{1/2}(\xi_e)}+\frac{F_{3/2}(\xi_h)}{F_{1/2}(\xi_h)}\right)+P(T,T_0) , \quad (8)$$

where τ_{rad} is the radiative recombination time and $P(T,T_0)$ is the power given by an electron-hole pair of the plasma at temperature T to the lattice at temperature T_0.

For densities and temperatures of interest here, the carriers and the lattice are coupled by acoustical phonons, via deformation potential and piezoelectric coupling. The most important effect is found to be the piezoelectric coupling of holes with the lattice.[18] In these conditions, it can be shown that the power exchanged with the lattice is a small fraction of the power given to the electron-hole plasma by the laser. Rewriting Eq. (8) with $P(T,T_0)=0$, we obtain a relation between $\eta=(h\nu-E_G)/kT$ and ξ_e (ξ_h).

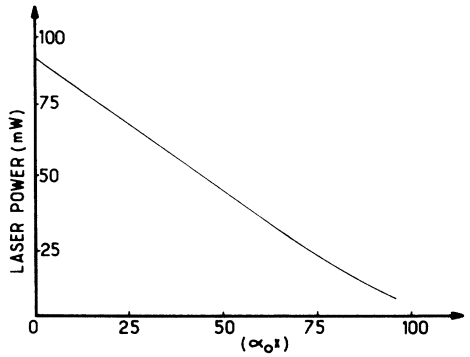

FIG. 6. Laser power plotted against the depth (in dimensionless unit) for the CO line $h\nu=238.6$ meV.

Equations (7) and (8) determine the dependence between $J(x)$ and $\xi_e(x)$. We neglect recombination processes at the surface ($x=0$); the electronic quasi-Fermi level $\xi_e(0)$ is then fixed only by the incident intensity of the laser beam. Equation (6) gives the spatial distribution $\xi_e(x)$ of the electronic quasi-Fermi level.

Figs. 6 and 7 show results for the particular CO line $h\nu=238.6$ meV ($\alpha_0=2\times10^3$ cm^{-1}). From the luminescence spectrum, a renormalized band-gap energy $E_G=232.5$ meV has been assumed. We find $\xi_e(0)=8.6$; $\xi_h=-1.69$; $\eta=7.04$; $kT=0.87$ meV; $n(0)=4.4\times10^{15}$ cm^{-3}; $1/\tau_{rad}=\gamma n=25$ ns for an incident intensity $I=7.8\times10^{21}$ cm^{-2} s^{-1} ($P=93$ mW). It can be noted that the electronic quasi-Fermi

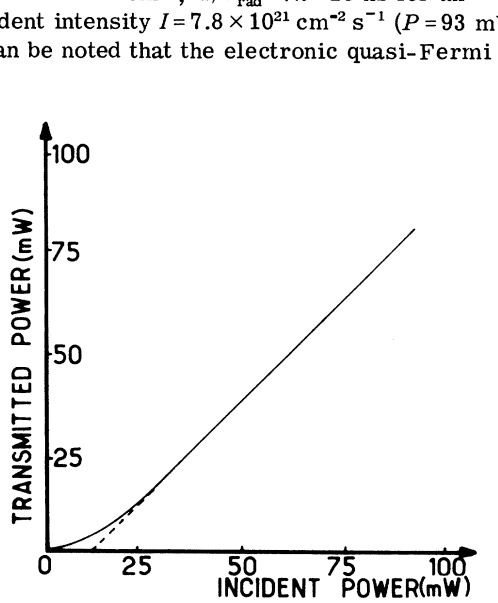

FIG. 7. Transmitted power vs incident power. This curve is obtained by determining in Fig. 6 for any incident power at $\alpha_0 x$, the transmitted power value at $\alpha_0 x+\alpha_0 d$. $d=60$ μm is the sample thickness; $\alpha_0=2\times10^3$ cm^{-1} is the absorption coefficient at low intensity.

level energy is larger than the kinetic energy of electrons at creation (of course, $\xi_e + \xi_h < \eta$).

Figure 6 shows the attenuation of the laser power inside sample. The power decreases linearly till a value $\alpha_0 x \sim 60$. In this range, the quasi-Fermi levels of electrons and holes remain nearly constant. Figure 7 shows the transmitted power as a function of the incident power for a sample thickness $d = 60\ \mu$m. The threshold is found to be 12 mW. At high power, the slope of the curve is nearly equal to one and the transmission rate is 85%. Experimentally, the threshold is 25 mW and the slope value is half the one obtained at great wavelength. As discussed above, inhomogeneity of the laser spot and uncertainties due to interference effect can explain the discrepancies between experimental and theoretical values.

The shape of the band-to-band recombination line is calculated by taking a constant density of carriers. Light emitted from depth x is attenuated or amplified before going out the sample. The amplification factor is $(1 - e^{-\alpha d})/\alpha d$, where α given by Eq. (4) takes into account the densities of carriers in conduction and valence bands. By summing light intensities emitted from different depths into the sample, we obtain the intensity $I(\eta)$ of the band-to-band recombination line

$$I(\eta) \sim \eta^{1/2} \left\{ \left[f_e\left(\eta \frac{\mu_{hh}}{m_e}\right) f_h\left(\eta \frac{\mu_{hh}}{m_{hh}}\right) \right] + \left(\frac{\mu_{lh}}{\mu_{hh}}\right)^{3/2} \left[f_e\left(\eta \frac{\mu_{lh}}{m_e}\right) f_h\left(\eta \frac{\mu_{lh}}{m_{lh}}\right) \right] \right\} \frac{1 - e^{-\alpha(\eta) d}}{\alpha(\eta) d}, \tag{9}$$

where we take

$$\alpha_0(\eta) = \alpha_0(\eta_L)(\eta/\eta_L)^{1/2},$$

with $\eta_L = (h\nu_L - E_G)/kT$ corresponding to the laser photon energy $h\nu_L$.

Results of the calculations can be seen in Fig. 3. The amplification factor has a weak wavelength dependence. Its maximum value, near $h\nu = 236$ meV, is 1.5; it corresponds to the beginning of stimulated emission in the sample. The band-to-band luminescence spectrum gives a distorted image of the carrier distribution function. Due to reabsorption or amplication of the light emitted by the sample, the peak of the band-to-band line is at lower energy than the CO- laser photon energy. This is in agreement with experiments. We must note that the quantitative interpretation of our previous experiments on optical pumping[19] must be revised since it did not take gain and reabsorption into account.

IV. ELECTRONIC POLARIZATION DEPENDENT TRANSMISSION

Since a spin orientation of electrons is partly achieved by optical pumping with circularly polarized light, the transmission of light may depend on its polarization (circular or linear). Experimentally, it is easier to modify the electronic polarization with a transverse magnetic field than to vary the light polarization without varying intensity. We use a square-wave modulated magnetic field and detect the power of the transmitted light at the same frequency. A weak variation ΔP_T of the transmitted circularly polarized light power P_T is observed: $\Delta P_T/P_T = 2 \times 10^{-3}$ for $h\nu = 238.6$ meV, $P_I = 80$ mW and $H = 3$ G (Fig. 8). The transmission is larger without magnetic field. No variation is observed when the light is linearly polarized. The model developed before allows us to calculate the effect of a transverse magnetic field on the transmission of circularly polarized light.

The two spin gases are described by two quasi-Fermi levels ξ^+ and ξ^- (in kT units) in a weak transverse magnetic field and by a common quasi-Fermi level ξ in high transverse magnetic field. The conservation equations now become

$$(\alpha_+ + \alpha_-)J(x) = r[n_+(x) + n_-(x)]^2, \tag{10}$$

$$(\alpha_+ - \alpha_-)J(x) = [n_+(x) - n_-(x)] \frac{1 + (\omega T_{1e})^2}{T_{1e}}. \tag{11}$$

n_+ and n_- are the electronic densities of up and down pairs; $\alpha_+ J$ and $\alpha_- J$ are their rates of creation; $\alpha_+ + \alpha_-$ is the absorption coefficient for circularly polarized light. The depolarization rate is $1/T_{1e} = 1/T_1 + r(n_+ + n_-)$, where T_1 is the spin relaxation time; ω is the Larmor frequency of electrons in the magnetic field H. It is worthwhile to note that the initial polarization of elec-

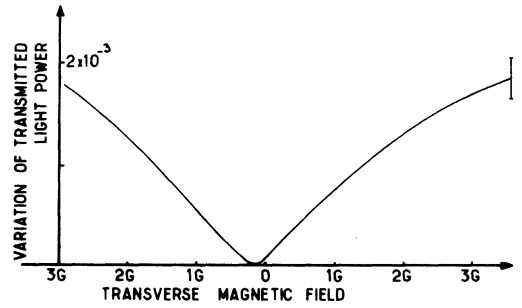

FIG. 8. Experimental relative variation of the transmitted light ($h\nu = 238.6$ meV, $P_I = 80$ mW) vs transverse magnetic field. The noise is indicated on the right-hand side of the curve. Asymmetry is due to local magnetic field.

trons is no longer equal to 0.5 but tends to zero for total saturation.

Since the steady-state electronic polarization is weak, we develop the previous equations to first order in quasi-Fermi level energy differences. For the sake of simplicity, the results which are given by complicated algebraic formula, will not be presented here. The curve of relative variation of transmitted light intensity with magnetic field is found to be a Lorentzian, whose width increases with the intensity of the incident light. In the limit of total saturation ($\xi = \xi_s$) the relative variation of transmitted intensity $\Delta I_T/I_T$ tends to zero as $(1/I_T)^2$. The differences $\Delta\xi^+ = \xi^+ - \xi_s$, $\Delta\xi^- = \xi^- - \xi_s$, and $\Delta\xi = \xi - \xi_s$ tend to zero as $1/I_T$ with following relations:

$$\Delta\xi^+/\Delta\xi^- = \tfrac{1}{3}, \quad \Delta\xi/\Delta\xi^- = \tfrac{1}{2}. \tag{12}$$

We give numerical results for the previous set of parametrers and $T_{1e}/\tau_{\text{rad}} = 0.1$:

$$\frac{\Delta I_T}{I_T} = \frac{5.35\times10^{-4}}{1+(\omega T_{1e}/2.15)^2}.$$

Figure 8 shows the experimental variation of transmission with magnetic field. The curve is nearly Lorentzian. Its maximum value is four times larger than the calculated value. This discrepancy is attributed to the important contribution of regions in the sample where saturation is not completely achieved. The experimental width is 1.5 G. It corresponds to a spin relaxation time $T_1 = 3$ nsec and a carrier lifetime $\tau = 30$ nsec, in good agreement with calculated value of radiative lifetime.

V. NONEQUILIBRIUM PLASMA

It is worthwhile to compare the value of the carrier density we obtain experimentally, with the one at the minimum energy per pair in the electron-hole plasma. The Hartree-Fock energy (E_{HF}) in Rydberg units is very similar in InSb and GaAs:

$$\frac{E_{\text{HF}}}{N} \cong 1.6/r_s^2 - 1.6/r_s \quad \text{for } N \text{ electrons}.$$

r_S is the interparticle distance in units of effective Bohr radius. Assuming the same correlation energy (in reduced units) in InSb and GaAs, we obtain the interparticle distance value $r_S^c = 1.5$ which gives the energy minimum of the plasma. The corresponding densities in InSb and GaAs are respectively, $n_c = 6\times10^{13}$ cm^{-3} and $n_c = 2\times10^{16}$ cm^{-3}.[20,21] In InSb, the densities we obtain, $n = 4.4\times10^{15}$ cm^{-3} ($r_s = 0.4$), are higher than n_c by two orders of magnitude. We emphasize we have here evidence of a nonequilibrium plasma steady state. Brinkman and Rice[20] predicted that in such a situation, the electron-hole gas would attempt to expand rapidly into the lower-density region. However, the behavior of the band-to-acceptor line at high excitation power shows that the transverse distribution of carriers is determined by the laser beam inhomogeneity. We conclude that the plasma expansion is less than the laser-spot diameter (200 μm).

Assuming that the optical transition occurs without change in the volume of the plasma,[22] one can see that the shift of the optical band gap is

$$\Delta E = \tfrac{4}{3}E_{\text{ex}} + E_{\text{corr}} + n\frac{\partial E_{\text{corr}}}{\partial n}, \tag{13}$$

where E_{ex} and E_{corr} are, respectively, exchange energy and correlation energy per pair in the plasma.

The exchange-energy contribution to the band-gap shift is $\frac{4}{3}E_{\text{ex}} = 2.2$ meV for $n = 4.4\times10^{15}$ cm^{-3} (Fig. 3). The correlation energy contribution is found to be a fraction of millielectronvolt.

ACKNOWLEDGMENTS

We would like to acknowledge stimulating discussions with J. P. Maneval who pointed out to us the importance of piezoelectric scattering of holes in InSb at low temperature. We would also like to thank P. Barnier and F. Yppert for their assistance in the measurements.

*Laboratoire associé au Centre National de la Recherche Scientifique.

[1]S. L. McCall and E. L. Hahn, Phys. Rev. 183, 457 (1969).
[2]F. Brückner *et al.*, Zh. Eksp. Teor. Fiz. 67, 2219 (1974) [Sov. Phys.-JETP 40, 1101 (1975)].
[3]S. Haroche and F. Hartmann, Phys. Rev. A 6, 1280 (1972).
[4]R. N. Zitter, Appl. Phys. Lett. 14, 73 (1969).
[5]J. Shah, R. F. Leheny, and C. Lin, Solid State Commun. 18, 1035 (1976).
[6]J. F. Reintjes, J. C. McGroddy, and A. E. Blakeslee, J. Appl. Phys. 46, 879 (1975).
[7]A. V. Nurmikko, Opt. Commun. 16, 365 (1976).
[8]J. C. Matter, A. L. Smirl, and M. O. Scully, Appl. Phys. Lett. 28, 507 (1976).
[9]C. J. Kennedy *et al.*, Phys. Rev. Lett. 32, 419 (1974); C. V. Shank and D. M. Auston, *ibid.* 34, 479 (1975); A. L. Smirl *et al.*, Opt. Commun. 16, 118 (1976).
[10]N. Menyuk, A. Pine, and A. Mooradian, IEEE J. Quantum Electron. QE-11, 477 (1975). The authors remarked that nonlinear transmission effects are

seen in longitudinal cw optical pumping of an InSb laser.

[11]A. Mooradian and H. Y. Fan, Phys. Rev. 148, 873 (1966).

[12]W. F. Brinkman and P. A. Lee, Phys. Rev. Lett. 31, 237 (1973).

[13]S. L. McCall, Phys. Rev. A 9, 1515 (1974). McCall showed that instabilities in light propagation may occur in absorbing media. We did not observe any effect.

[14]In steady state, the ratio ρ of neutral and ionized acceptors is fixed by the equality of the recombination rate of electrons on neutral acceptors and of the trapping rate of holes on ionized acceptors. Since these two rates are proportional to carrier density, the ratio ρ is independent of the excitation intensity.

[15]H. J. Fossum and B. Ancker-Johnson, Phys. Rev. B 8, 2850 (1973). The authors have studied the radiative recombination of electron-hole pairs generated by two-photon absorption in InSb. The observed excess conductivity decay gives a value of r, the bimolecular recombination constant, one or two orders of magnitude smaller than the theoretical values. But, in our opinion, these authors did not take into account correctly the effect of reabsorption. Because of the high refractive index of InSb ($n = 4$) only 1% of the emitted light which reaches the surface can escape out of the sample, so that almost all the radiation is reabsorbed several times before going out of the sample. This effect would reconcile experimental and theoretical values of the bimolecular constant. In our experiment, it is not necessary to take into account reabsorption, since the light emitted from the excited volume of the sample is reabsorbed outside this volume and creates electron-hole pairs which do not contribute to the saturation.

[16]This expression of the rate of radiative recombination is justified, as shown by Fossum and Ancker-Johnson (see Ref. 15) if the hole distribution is not degenerate. We verified that, under our conditions, the error is less than 10%.

[17]The order of magnitude of τ_ϵ can be evaluated from the value of the momentum relaxation time τ_k due to electron-hole collisions: $1/\tau_\epsilon \sim (1/\tau_k)(4m_e/m_h)$, where m_e and m_h are electron and hole masses. By analogy with scattering on ionized impurities, τ_k and τ_ϵ are calculated to be, respectively, 10^{-12} sec and 5×10^{-12} sec for $p = 10^{15}$ cm^{-3}. This is to be compared with the radiative-lifetime value, 100 nsec.

[18]Calculation of the scattering of energy by a piezoelectric potential can be done with formula given by Kogan [S. M. Kogan, Sov. Phys.-Solid State 4, 1813 (1963)]. The appropriate value of the piezoelectric modulus is $e_{14} = 2.13\times10^4$ (dyn)$^{1/2}$ cm^{-1} [G. Arlt and P. Quadflieg, Phys. Status Solidi 25, 323 (1968)].

[19]R. Bichard, P. Lavallard, and C. Benoît à la Guillaume, *Proceedings of the Twelfth International Conference on the Physics of Semiconductors, Stuttgart*, edited by M. H. Pilkuhn (Teubner, Stuttgart, 1974), p. 766.

[20]M. Combescot and P. Nozières, J. Phys. C 5, 2369 (1972).

[21]W. F. Brinkman and T. M. Rice, Phys. Rev. B 7, 1508 (1973).

[22]V. G. Lysenko, V. I. Revenko, T. G. Tratas, and V. B. Timofeev, Zh. Eksp. Teor. Fiz. 68, 335 (1975) [Sov. Phys.-JETP 41, 163 (1975)].